Imidazolate-bridged Copper(II) Complexes with Infinite Zigzag-chain and Tetranuclear Structures formed by Deprotonation and Self-assembly†

Naohide Matsumoto,* Takeshi Nozaki, Hiroyuki Ushio, Ken-ichiro Motoda, Masaaki Ohba, Genjin Mago and Hisashi Ōkawa
Department of Chemistry, Faculty of Science, Kyushu University, Hakozaki, Higashi-ku, Fukuoka 812, Japan

A method of molecular design of self-assembling metal complexes has been established. The copper(II) complex with a quadridentate ligand $[Cu(HL^2)]ClO_4$ undergoes deprotonation of the imidazole proton under basic conditions to give an imidazolate-bridged polymeric compound $[(CuL^2)_\infty]$, where H_2L^2 = *N*-3-ethoxysalicylidene-*N*′-imidazol-4-ylmethylenecyclohexane-1,2-diamine. The latter compound crystallizes in the monoclinic space group $P2_1/a$ with $a = 15.515(5)$, $b = 9.338(5)$, $c = 12.660(2)$ Å, $\beta = 95.33(2)°$, and $Z = 4$, $R = 0.078$ for 1721 reflections. It has an infinite zigzag-chain structure and the variable-temperature magnetic data are well reproduced using the Ising model based on $H = -2\Sigma J_{ij}S_iS_j$ with a J value of -1.8 cm^{-1}. The complex $[Cu(HL^3)Cl]ClO_4$ with a tridentate ligand gives an imidazolate-bridged tetranuclear complex $[(CuL^3)_4][ClO_4]_4$ on deprotonation at the imidazole nitrogen, where HL^3 = *N*-imidazol-4-ylmethylene-*N*′,*N*′-dimethylpropane-1,3-diamine. The latter compound crystallizes in the triclinic space group $P\bar{1}$ with $a = 15.216(6)$, $b = 15.592(5)$, $c = 15.102(5)$ Å, $\alpha = 104.98(3)°$, $\beta = 108.44(3)°$, $\gamma = 61.12(2)°$, $Z = 2$, and $R = 0.096$ for 6931 reflections. The structure consists of a cyclic tetranuclear mclecule in which each imidazolate nitrogen atom co-ordinates axially to the copper(II) ion of the adjacent unit. Variable-temperature magnetic data are well reproduced using the Heisenberg model based on $H = -2J(S_1 \cdot S_2 + S_2 \cdot S_3 + S_3 \cdot S_4 + S_4 \cdot S_1)$ with $J = -60.0$ cm^{-1}.

The design of molecular architecture by self-assembly processes has received much attention from several viewpoints such as the development of functional materials[1] and construction of single- and double-helix structures.[2] A feature of self-assembly is the use of modular building blocks that contain sufficient structural information to guide the self-assembly reaction.[3,4] In order to be a self-assembling molecule a complex should satisfy the following conditions: (1) it should have a co-ordinating ability to other metal ions and (2) at the same time be able to receive a donor atom; (3) the relative orientation between adjacent linked metal complexes should be variable in order to form a variety of shapes; (4) a construction process from building blocks to a self-assembled molecule, and the reverse disassembly process, should be available.

We have been interested in metal complexes containing an imidazole moiety.[5,6] Such complexes exist as a monomer in the form of the protonated species under acidic conditions, while under basic conditions a deprotonated imidazolate nitrogen atom can function as a ligand and co-ordinate to another metal ion. When, in addition, the complex has a vacant or a substitutable co-ordination site, a self-assembly reaction will occur. A variety of structures of assembled molecules can occur by choosing appropriate ligand frameworks or metal ions. It is also expected that the construction and disassembly of the assembled molecule can be reversible depending on the pH.

Previously we reported that the mononuclear copper(II) complex **1a** undergoes deprotonation of the imidazole proton under basic conditions to give a unique helical chain structure by self-assembly as depicted in Fig. 1.[6a] In the helical structure, each deprotonated imidazolate nitrogen co-ordinates axially to the copper(II) ion of the adjacent unit to afford a tetragonal-pyramidal co-ordination geometry about each copper(II) ion. It can be rationalized that the helical structure is derived from co-operative demands of the planar quadridentate ligand and square-pyramidal co-ordination geometry of the copper(II) ion. If either the ligand framework or metal ion is changed, different types of self-assembled structures may be formed. We selected **2a** and **3a** and studied the structures of the deprotonated forms **2b** and **3b**.

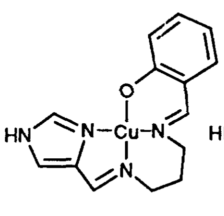

1a $[Cu(HL^1)]^+$

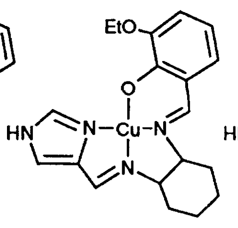

2a $[Cu(HL^2)]^+$

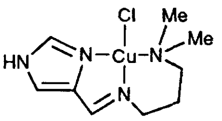

3a $[Cu(HL^3)Cl]^+$

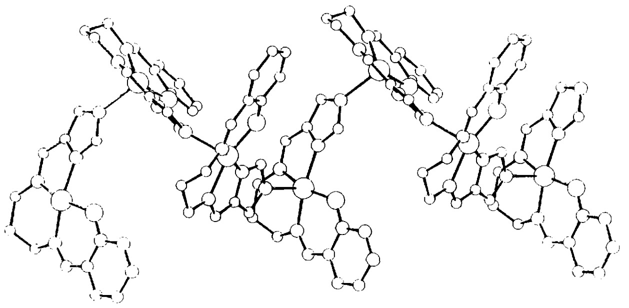

Fig. 1 Crystal structure of $[(CuL^1)_\infty]$ **1b** showing a unique helical structure

---

† *Supplementary data available* (No. SUP 56953, 4 pp.): magnetic susceptibilities and pH titration curve. See Instructions for Authors, *J. Chem. Soc., Dalton Trans.*, 1993, Issue 1, pp. xxiii–xxviii.

Experimental

CAUTION: Perchlorite salts are potentially explosive and should only be handled in small quantities.

Materials.—All chemicals and solvents used for the synthesis were reagent grade. Reagents used for the physical measurements were of spectroscopic grade. 4-Formylimidazole was prepared according to the literature method.[7]

$[Cu(HL^2)]ClO_4$ **2a**. To a solution of *trans*-cyclohexane-1,2-diamine (1.12 g, 10 mmol) in chloroform (100 cm^3) was added dropwise 3-ethoxysalicylaldehyde (1.50 g, 10 mmol) in chloroform (50 cm^3). The resulting solution was kept for *ca.* 1 week at room temperature and then the volume reduced to give an oily material. This was dissolved in methanol (20 cm^3) and the solution was mixed with 4-formylimidazole (0.96 g, 10 mmol) in methanol (20 cm^3). The mixture was warmed on a water-bath at 50 °C for 30 min and then cooled to room temperature. A solution of $Cu(ClO_4)_2{\cdot}6H_2O$ (3.71 g, 10 mmol) in methanol (30 cm^3) was added, immediately precipitating microcrystalline material. The crystals were filtered off, washed with methanol and diethyl ether, and then dried *in vacuo*, Λ_M 150 S cm^2 mol^{-1} in MeCN, λ_{max} in methanol 581 nm (ε = 210 dm^3 mol^{-1} cm^{-1}) IR data (cm^{-1}): 3250 ν(N–H), 1640 ν(C=N), 1150 and 1080 ν(Cl–O) {Found: C, 44.90; H, 4.75; Cu, 12.45; N, 10.80. Calc. for $[Cu(HL^2)]ClO_4{\cdot}MeOH$, $C_{19}H_{23}ClCuN_4O_6$: C, 44.95; H, 5.10; Cu, 11.90; N, 10.50%).

$[(CuL^2)_\infty]$ **2b**. Compound **2a** was dissolved in dimethylformamide (dmf) and then filtered. To the filtrate was added a dmf solution of triethylamine (1.52 g, 15 mmol), immediately precipitating a green microcrystalline material. Compound **2b** is insoluble even in dmf and Me_2SO, λ_{max} in reflectance spectrum 645 nm. IR data (cm^{-1}): disappearance of 3250 ν(N–H), 1150 and 1080 ν(Cl–O); 1640 ν(C=N) (Found: C, 56.20; H, 5.50; Cu, 15.75; N, 13.70. Calc. for $C_{19}H_{23}CuN_4O_2$: C, 56.65; H, 5.75; Cu, 15.35; N, 13.90%).

$[Cu(HL^3)Cl]ClO_4$ **3a**. To a solution of 4-formylimidazole (0.96 g, 10 mmol) in methanol (20 cm^3) was added *N,N*-dimethylpropane-1,3-diamine (1.02 g, 10 mmol) in methanol (20 cm^3) and the mixture was stirred for 1 h at room temperature. The salt $CuCl_2{\cdot}H_2O$ (1.70 g, 10 mmol) in methanol (10 cm^3) was added and subsequently $NaClO_4$ (1.22 g, 10 mmol) in methanol (10 cm^3). The resulting blue solution was filtered and the filtrate allowed to stand for several days. The precipitated blue crystals were filtered off, washed with diethyl ether, and dried in air, Λ_M 150 S cm^2 mol^{-1} in MeCN, λ_{max} in MeCN 671 nm (ε = 90 dm^3 mol^{-1} cm^{-1}). IR data (cm^{-1}): 3200 ν(N–H); 1630 ν(C=N); 1140 and 1110 ν(Cl–O) (Found: C, 24.35; H, 3.90; Cu, 13.95; N, 12.50. Calc. for $C_{25}H_{27}Cl_2CuN_6O_6$: C, 24.40; H, 3.65; Cu, 14.35; N, 12.65%).

$[(CuL^3)_4][ClO_4]_4$ **3b**. To a solution of complex **3a** in water–methanol was added triethylamine and the mixture adjusted to pH 9–10. After standing for several days, deep blue crystals appeared. They were filtered off and dried in air, Λ_M 120 S cm^2 mol^{-1} in MeCN, λ_{max} in MeCN 607 nm (ε = 170 dm^3 mol^{-1} cm^{-1}). IR data (cm^{-1}): disappearance of 3200 ν(N–H); 1630 ν(C=N); 1140 and 1110 ν(Cl–O) (Found: C, 31.60; H, 4.35; Cu, 17.90; N, 16.40. Calc. for $C_{36}H_{60}Cl_4Cu_4N_{16}O_{16}$: C, 31.60; H, 4.40; Cu, 18.55; N, 16.35%).

Physical Measurements.—Elemental analyses for C, H and N were performed at the Elemental Analysis Service Center of Kyushu University. Copper analyses were made on a Shimadzu AA-680 atomic absorption/flame emission spectrophotometer. Infrared spectra were measured on KBr disks with a JASCO IR-810 spectrophotometer. Electrical conductivity measurements were carried out on a Denki Kagaku Keiki AOL-10 digital conductometer in *ca.* 10^{-3} mol dm^{-3} solutions. pH Titrations were carried out at 25 °C with a Beckman Φ50 pH meter. Electronic spectra were measured on a Shimadzu MPS-2000 multipurpose recording spectrophotometer. Magnetic susceptibilities were measured with a HOXAN HSM-D SQUID susceptometer in the temperature range 4.2–100 K and with a Faraday balance in the temperature range 80–300 K. The calibration was made with $Mn(NH_4)_2(SO_4)_2{\cdot}6H_2O$ for the SQUID susceptometer[8] and with $[Ni(en)_3][S_2O_3]$ (en = ethane-1,2-diamine) for the Faraday balance.[9] Diamagnetic corrections were made with Pascal's constants.[10] Effective magnetic moments were calculated by the equation $\mu_{eff} = 2.828(\chi_A T)^{\frac{1}{2}}$, where χ_A is the magnetic susceptibility per copper.

X-Ray Crystallographic Studies.—Single crystals of complex **2b** suitable for X-ray analysis were obtained by a diffusion method using an H-tube, where the dmf solution of **2a** and methanol solution of triethylamine were used. The crystal was mounted on a glass fibre and coated with epoxy resin. Since crystals of **3b** easily effloresce, the crystal used for X-ray analysis was sealed in a glass capillary containing a small amount of mother-liquor. X-Ray data for both compounds were collected on a Rigaku Denki AFC-5 four-circle automated diffractometer with graphite-monochromatized Mo-Kα radiation at ambient temperature. The unit-cell parameters were determined from 25 reflections in the range $20 \leqslant 2\theta \leqslant 30°$. Standard reflections were monitored every 100 and showed good stability. Intensity data were corrected for Lorentz and polarization effects but no absorption correction was applied. The details of data collection, crystallographic data, and data reduction are summarized in Table 1.

The structures were solved by the standard heavy-atom method and refined by block-diagonal least squares. Reliability factors were defined as $R = \Sigma||F_o| - |F_c||/\Sigma|F_o|$ and the function minimized was $R' = [\Sigma w(|F_o| - |F_c|)^2/\Sigma|F_o|^2]^{\frac{1}{2}}$, where in the final least-squares calculation the weighting scheme $w = 1/\sigma(F)$ was used. Neutral atomic scattering factors were taken from the literature.[11] The hydrogen atoms were inserted at the calculated positions. The hydrogen atoms of **2b** were refined with isotropic thermal parameters, but those of **3b** were not refined. Final Fourier difference syntheses were featureless. The computation was carried out on a FACOM V-100 computer at the Computer Center of Kyushu University using the UNICS III program system.[12a,b] Positional parameters of the non-hydrogen atoms of **2b** and **3b** are given in Tables 2 and 3, respectively.

Additional material available from the Cambridge Crystallographic Data Centre comprises H-atom coordinates, thermal parameters and remaining bond lengths and angles.

Results and Discussion

Mononuclear copper(II) complexes **2a** and **3a** satisfy the conditions (1)–(4) for self-assembling molecules described earlier. Both complexes contain an imidazole group in their ligands and each of the nitrogen atoms of the imidazole can co-ordinate to other metal complexes under basic conditions. Complex **2a** adds a donor atom at the axial co-ordination site; in **3a** an imidazolate nitrogen atom of another unit can be substituted for the chloride. The difference in the ligand framework between **2a** and **3a** can produce a different relative orientation of the adjacent molecule between **2a** and **3a**. It is expected that the self-assembled polynuclear structure and the protonated monomer can be interconverted reversibly depending on the pH.

When complexes **2a** and **3a** were treated with base (pH 9–10) the deprotonated imidazolate nitrogen co-ordinated to the metal ions of another unit to form self-assembled compounds **2b** and **3b**, respectively. The ν(N–H) vibration, observed at 3250 and 3200 cm^{-1} for their precursor compounds **2a** and **3a**, is absent in the IR spectra of **2b** and **3b**. The d–d band maxima in the absorption spectra are shifted from 581 nm for **2a** to 645 nm for **2b** after deprotonation, indicating a difference in their co-ordination geometries. The corresponding values for **3a** and **3b** are 671 and 607 nm, respectively. Compound **2b** is insoluble in common solvents, while **3b** is moderately soluble, owing to their structures (infinite polymer **2b** and tetramer **3b**)

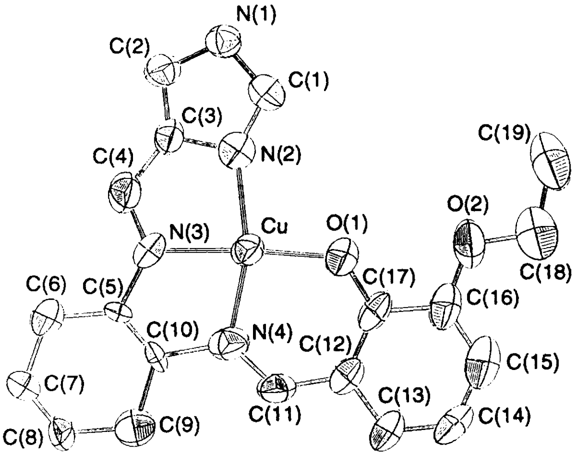

Fig. 2 An ORTEP drawing of the asymmetrical unit of $[(CuL^2)_\infty]$ **2b** showing the atom numbering scheme (thermal ellipsoids at 50% probability level)

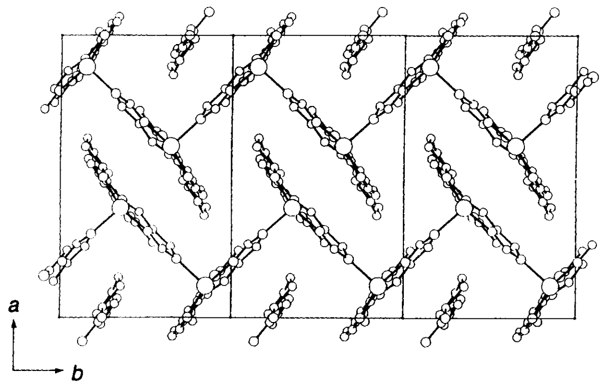

Fig. 3 View of $[(CuL^2)_\infty]$ **2b** projected along the *c* axis showing an infinite zigzag chain structure

Table 1 Crystallographic data for $[(CuL^2)_\infty]$ **2b** and $[(CuL^3)][ClO_4]_4 \cdot 2H_2O \cdot 2MeOH$ **3b**

	2b	**3b**
Formula	$C_{19}H_{23}CuN_4O_2$	$C_{38}H_{72}Cl_4Cu_4N_{16}O_{20}$
M	402.96	1469.12
Crystal system	Monoclinic	Triclinic
Space group	$P2_1/a$	$P1$
a/Å	15.515(5)	15.216(6)
b/Å	9.338(5)	15.592(5)
c/Å	12.660(2)	15.102(5)
α/°	90	104.98(3)
β/°	95.33(2)	108.44(3)
γ/°	90	61.12(2)
U/Å^3	1826.3	2952.0
Z	4	2
D_c/g cm^{-3}	1.465	1.653
D_m/g cm^{-3}	1.45	1.62
F(000)	840	1512
μ (Mo-Kα)/cm^{-1}	12.71	16.88
Crystal size/mm	0.1 × 0.1 × 0.2	0.4 × 0.4 × 0.3
No. of data used	1721	6931
R	0.078	0.096
R′	0.038	0.094

Table 2 Atomic coordinates of $[(CuL^2)_\infty]$ **2b**

Atom	*x*	*y*	*z*
Cu	1114(1)	1477(1)	234(1)
O(1)	1107(3)	1255(6)	1745(4)
O(2)	1459(4)	928(7)	3751(4)
N(1)	2943(4)	−1812(7)	−374(5)
N(2)	1956(4)	−127(7)	−52(5)
N(3)	839(4)	1372(8)	−1321(5)
N(4)	1(5)	2491(8)	43(5)
C(1)	2587(6)	−973(8)	365(6)
C(2)	2493(5)	−1457(10)	−1311(6)
C(3)	1895(5)	−416(9)	−1136(6)
C(4)	1258(5)	376(10)	−1779(6)
C(5)	163(6)	2272(13)	−1754(6)
C(6)	−130(5)	2185(10)	−2889(6)
C(7)	−887(6)	3066(13)	−3185(6)
C(8)	−1398(6)	3433(16)	−2517(7)
C(9)	−1098(5)	3546(10)	−1353(6)
C(10)	−366(6)	2520(13)	−1096(6)
C(11)	−419(5)	2922(9)	849(6)
C(12)	−144(5)	2739(10)	1953(6)
C(13)	−666(6)	3362(12)	2657(6)
C(14)	−479(6)	3214(12)	3704(6)
C(15)	236(7)	2425(12)	4093(6)
C(16)	754(5)	1757(10)	3438(6)
C(17)	582(5)	1901(9)	2331(6)
C(18)	1632(6)	606(11)	4825(8)
C(19)	2360(7)	−403(12)	4960(9)

as described in the X-ray analysis section. Interconversion between **3a** and **3b** can be reversibly achieved by varying the pH of the solution, deprotonation of the imidazole group is being observed at pH 9 (see SUP 56953).

Structure of Complex **2b**.—An ORTEP[12c] drawing of complex **2b** with the atom numbering scheme is shown in Fig. 2. A view projected along the *c* axis is given in Fig. 3. Relevant interatomic bond distances and angles are given in Table 4.

As depicted in Fig. 3, compound **2b** assumes an infinite zigzag chain structure, where neighbouring units in the chain are related by a two-fold screw axis along *b*. Each copper(II) ion assumes a square-pyramidal co-ordination geometry in which the basal co-ordination plane is occupied by N_3O donor atoms of the quadridentate ligand with Cu–O and Cu–N bond distances of 1.925(5)–2.042(7) Å and the apical site is occupied by an imidazolate nitrogen of an adjacent unit with Cu–N 2.162(6) Å. The present structure is similar to the helical structure of **1b**.[6a] Both of these precursor compounds assume a square-planar co-ordination geometry and both of their deprotonated compounds assume a five-co-ordinate square-pyramidal geometry.

Structure of Complex **3b**.—An ORTEP drawing of complex **3b** with the atom numbering scheme is shown in Fig. 4. Relevant interatomic distances and angles are given in Table 5. Compound **3b** assumes an imidazolate-bridged cyclic tetranuclear structure in which four copper(II) ions are tetrahedrally arranged. Those Cu···Cu distances with linkage through the imidazolate group [6.042(3)–6.067(3) Å] are shorter than those without linkage [6.757(3), 7.124(3) Å], indicating a distortion of the Cu_4 core from an ideal tetrahedron. Each copper(II) ion assumes a square-planar co-ordination geometry in which three nitrogen donor atoms of the tridentate ligand and the imidazolate nitrogen of the adjacent unit occupy the four equatorial co-ordination sites. The Cu–N bond distances around each copper(II) ion are within the range 1.98(2)–2.10(2) Å. The dihedral angles between the neighbouring co-ordination planes are 80.1, 74.6, 65.0 and 84.1° for those involving Cu(1), Cu(2); Cu(2), Cu(3); Cu(3), Cu(4); and Cu(1), Cu(4) respectively. It should be noted that this type of tetrameric structure has been postulated on the basis of molecular modelling and magnetic analysis of a deprotonated copper(II) complex with a tridentate ligand derived from the condensation of histamine (imidazole-4-ethanamine) and salicylaldehyde.[5]

Magnetic Susceptibility Studies.—The magnetic behaviour of

Table 3 Atomic coordinates of $[(CuL^3)_4][ClO_4]_4\cdot 2H_2O\cdot 2MeOH$ **3b**

Atom	*x*	*y*	*z*
Cu(1)	3 399(1)	3 171(1)	3 752(1)
Cu(2)	6 685(1)	3 153(1)	2 306(1)
Cu(3)	7 373(1)	−980(1)	2 420(1)
Cu(4)	7 502(1)	1 159(1)	6 400(1)
N(1)	5 996(7)	1 758(7)	5 834(6)
N(2)	4 584(7)	2 495(7)	4 741(6)
N(3)	2 842(7)	2 390(7)	4 103(7)
N(4)	2 240(8)	3 620(8)	2 571(7)
C(1)	5 547(9)	2 382(9)	5 178(9)
C(2)	5 318(9)	1 413(9)	5 791(8)
C(3)	4 433(9)	1 892(9)	5 121(9)
C(4)	3 471(9)	1 832(10)	4 731(9)
C(5)	1 851(9)	2 328(10)	3 692(11)
C(6)	1 498(11)	2 506(12)	2 678(11)
C(7)	1 299(10)	3 524(13)	2 545(11)
C(8)	2 653(12)	2 963(13)	1 738(10)
C(9)	1 898(12)	4 652(13)	2 522(12)
N(5)	4 263(7)	3 620(7)	3 416(7)
N(6)	5 555(7)	3 414(7)	2 881(6)
N(7)	6 365(8)	4 551(7)	2 889(7)
N(8)	7 922(8)	2 923(8)	1 829(7)
C(10)	5 006(9)	2 987(9)	2 927(9)
C(11)	4 396(9)	4 454(9)	3 696(8)
C(12)	5 182(8)	4 335(8)	3 352(8)
C(13)	5 662(9)	4 931(9)	3 360(9)
C(14)	6 834(12)	5 179(10)	2 852(10)
C(15)	7 819(18)	4 542(16)	2 640(19)
C(16)	8 064(16)	3 821(13)	1 931(14)
C(17)	7 808(13)	2 544(13)	834(11)
C(18)	8 852(11)	2 134(14)	2 309(15)
N(9)	6 907(7)	1 757(7)	1 929(7)
N(10)	7 168(7)	285(6)	2 139(6)
N(11)	6 767(7)	−1 122(7)	1 018(6)
N(12)	7 993(8)	−2 469(8)	2 498(7)
C(19)	7 248(8)	1 112(8)	2 548(8)
C(20)	6 575(9)	1 298(9)	1 079(9)
C(21)	6 734(9)	423(9)	1 194(8)
C(22)	6 544(9)	−366(9)	617(8)
C(23)	6 511(11)	−1 939(10)	464(9)
C(24)	7 358(12)	−2 905(10)	751(9)
C(25)	7 482(12)	−3 033(10)	1 730(10)
C(26)	7 883(15)	−2 649(11)	3 386(11)
C(27)	9 103(12)	−2 906(11)	2 431(13)
N(13)	7 832(7)	−609(7)	3 786(6)
N(14)	7 716(7)	247(7)	5 204(6)
N(15)	9 072(7)	515(7)	6 688(6)
N(16)	7 370(8)	2 250(7)	7 560(7)
C(28)	7 200(9)	25(8)	4 350(8)
C(29)	8 818(9)	−794(9)	4 315(8)
C(30)	8 754(9)	−285(9)	5 176(8)
C(31)	9 446(9)	−97(9)	6 008(8)
C(32)	9 781(10)	692(11)	7 574(9)
C(33)	9 291(11)	1 749(11)	8 006(9)
C(34)	8 344(11)	2 007(10)	8 345(8)
C(35)	6 563(11)	2 394(11)	7 998(9)
C(36)	7 056(12)	3 180(10)	7 250(10)
Cl(1)	5 267(3)	5(3)	7 729(2)
O(1)	4 252(7)	685(7)	7 316(6)
O(2)	5 254(9)	−644(10)	8 187(11)
O(3)	5 893(9)	−387(10)	7 093(9)
O(4)	5 659(10)	582(12)	8 516(10)
Cl(2)	8 118(2)	2 767(2)	5 040(2)
O(5)	7 225(10)	3 623(10)	5 108(10)
O(6)	8 216(14)	2 625(15)	4 125(11)
O(7)	7 885(20)	2 071(14)	5 110(15)
O(8)	8 845(12)	2 816(16)	5 799(13)
Cl(3)	9 232(5)	4 106(4)	9 972(4)
O(9)	9 690(19)	3 157(16)	10 333(17)
O(10)	8 269(17)	4 375(22)	9 459(21)
O(11)	9 939(17)	3 993(18)	9 509(20)
O(12)	9 327(17)	4 807(12)	10 729(12)
Cl(4)	0(0)	5 000(0)	5 000(0)
O(13)	1 073(14)	4 392(15)	5 180(15)
O(14)	−276(33)	4 393(33)	5 259(35)
O(15)	120(38)	4 912(22)	4 150(26)
O(16)	−135(26)	4 046(34)	4 565(35)
O(W1)	2 592(7)	4 550(6)	4 750(6)
O(W2)	7 593(8)	37(7)	7 232(7)
O(M1)	1 043(6)	613(6)	416(5)
C(M1)	923(15)	491(15)	1 094(13)
O(M2)	4 482(6)	4 419(6)	425(6)
C(M2)	5 419(11)	3 759(11)	796(9)

Table 4 Selected bond distances (Å) and angles (°) of $[(CuL^2)]_\infty$ **2b**. Numbers in parentheses are estimated standard deviations (e.s.d.s) with least significant digits

Cu–N(2)	1.925(5)	Cu–N(3)	2.042(7)
Cu–N(4)	1.978(6)	Cu–O(1)	1.964(7)
Cu–N(1^I)	2.162(6)		
O(1)–Cu–N(2)	99.2(3)	N(2)–Cu–N(3)	82.5(3)
N(3)–Cu–N(4)	78.2(3)	N(4)–Cu–O(1)	95.1(3)

Symmetry relation: I $\frac{1}{2} - x, \frac{1}{2} + y, z$.

Table 5 Selected bond distances (Å) and angles (°) of $[(CuL^3)]_4[ClO_4]_4\cdot 2H_2O\cdot 2MeOH$ **3b**. Numbers in parentheses are e.s.d.s with least significant digits

Cu(1) ··· Cu(2)	6.042(3)	Cu(2) ··· Cu(3)	6.050(3)
Cu(3) ··· Cu(4)	6.067(3)	Cu(4) ··· Cu(1)	6.048(3)
Cu(1) ··· Cu(3)	6.757(3)	Cu(2) ··· Cu(4)	7.124(3)
Cu(1)–N(2)	2.01(1)	Cu(1)–N(3)	2.06(2)
Cu(1)–N(4)	2.02(2)	Cu(1)–N(5)	2.05(2)
Cu(2)–N(6)	2.03(2)	Cu(2)–N(7)	2.00(1)
Cu(2)–N(8)	2.06(1)	Cu(2)–N(9)	2.02(2)
Cu(3)–N(10)	1.98(2)	Cu(3)–N(11)	2.02(1)
Cu(3)–N(12)	2.05(2)	Cu(3)–N(13)	1.98(1)
Cu(4)–N(1)	2.00(1)	Cu(4)–N(14)	2.01(1)
Cu(4)–N(15)	2.06(2)	Cu(4)–N(16)	2.10(2)
N(2)–Cu(1)–N(3)	79.3(7)	N(3)–Cu(1)–N(4)	98.2(8)
N(4)–Cu(1)–N(5)	91.0(8)	N(2)–Cu(1)–N(5)	89.7(7)
N(6)–Cu(2)–N(7)	81.2(8)	N(7)–Cu(2)–N(8)	94.8(8)
N(8)–Cu(2)–N(9)	94.0(7)	N(6)–Cu(2)–N(9)	89.1(5)
N(10)–Cu(3)–N(11)	80.7(7)	N(11)–Cu(3)–N(12)	93.8(6)
N(12)–Cu(3)–N(13)	95.0(6)	N(10)–Cu(3)–N(13)	91.4(6)
N(1)–Cu(4)–N(14)	88.9(5)	N(14)–Cu(4)–N(15)	80.0(6)
N(15)–Cu(4)–N(16)	96.9(6)	N(1)–Cu(4)–N(16)	92.9(6)

complexes **2b** and **3b** is shown in Fig. 5 and 6, respectively, in the forms of plots of χ_A *vs.* *T* and μ_{eff} *vs.* *T*, where χ_A is the magnetic susceptibility per copper, μ_{eff} is the effective magnetic moment per copper, and *T* is the absolute temperature. The plot of $1/\chi_A$ *vs.* *T* for **2b** is linear and obeys the Curie–Weiss law [$1/\chi_A = (T - \theta)/C$] with a Weiss constant of $\theta = -8.5$ K, suggesting a weak antiferromagnetic interaction. The μ_{eff} is 1.98 μ_B at 290 K which is compatible with the spin-only value of 1.73 μ_B for $S = \frac{1}{2}$. As the temperature is lowered, μ_{eff} gradually decreases to 1.57 μ_B at 4.2 K. The magnetic susceptibility data were analysed on the basis of the Ising model for a one-dimensional infinite chain structure, equation (1), where the spin Hamiltonian in the form $H = -2\Sigma J_{ij}S_iS_j$ is used[13] and $K = J/kT$. The symbols have their usual meanings, $N\alpha$ denoting the temperature-independent paramagnetism. The observed susceptibility data were fitted by a least-squares method, where the disagreement factor $R =$

$$\chi_A = \frac{Ng^2\beta^2}{12kT}\cdot\frac{e^{4K} + (2 + K^{-1})e^{2K} - K^{-1}e^{-2K} + 5}{e^{2K} + e^{-2K} + 2} + N_\alpha \quad (1)$$

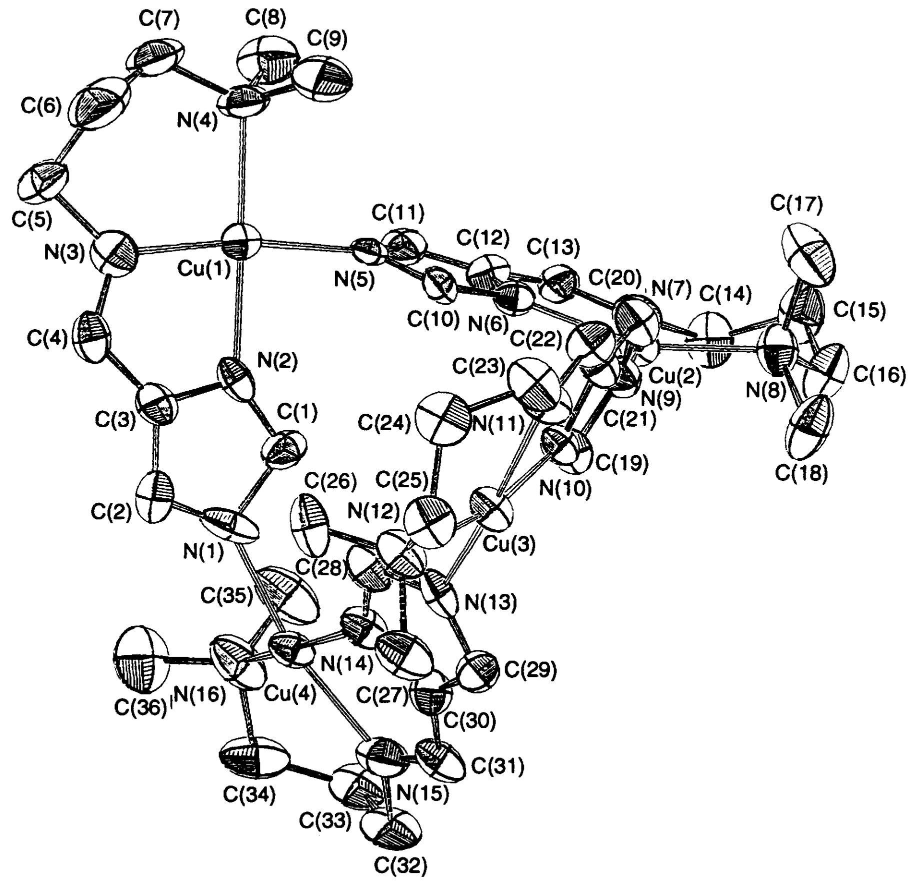

Fig. 4 An ORTEP drawing of $[(CuL^3)_4][ClO_4]_4$ **3b** showing the atom numbering scheme (thermal ellipsoids at 50% probability level)

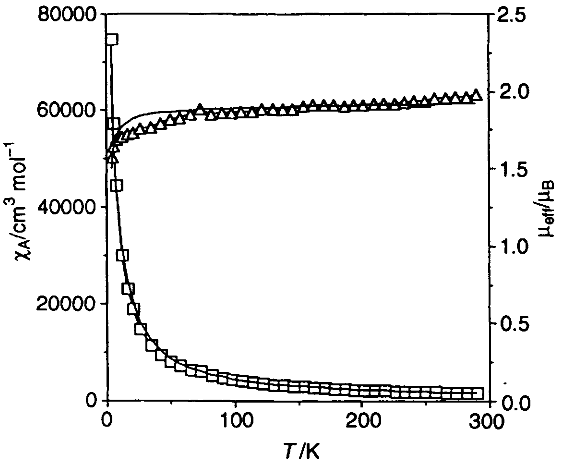

Fig. 5 Temperature dependences of magnetic susceptibility χ_A(□) and effective magnetic moment μ_{eff}(△) per copper of a polycrystalline sample of $[(CuL^2)_\infty]$ **2b**. Solid lines represent theoretical curves calculated using equation (1) with the best-fit parameters

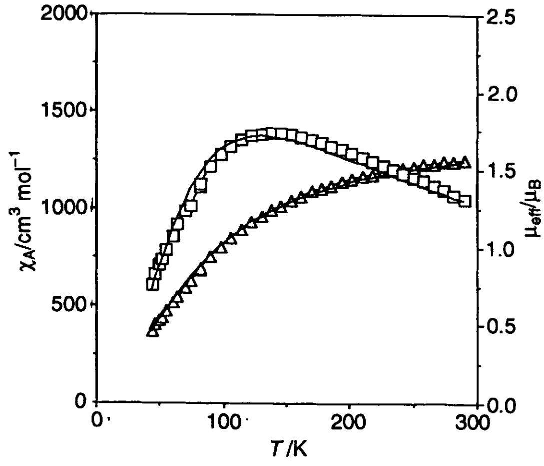

Fig. 6 Temperature dependences of magnetic susceptibility χ_A(□) and effective magnetic moment μ_{eff}(△) per copper of a polycrystalline sample of $[(CuL^3)_4][ClO_4]_4$ **3b**. Solid lines represent theoretical curves calculated using equation (2) with the best-fit parameters

$[\Sigma(\mu_{obs} - \mu_{calc})^2/\Sigma\mu_{obs}^2]^{\frac{1}{2}}$ was minimized and $N\alpha$ was fixed at 60×10^{-6} cm^3 mol^{-1}. The best-fit parameters $J = -1.8$ cm^{-1}, $g = 2.18$ and $R = 0.020$ were obtained. The calculated χ_A and μ_{eff} curves with the fitting parameters are represented by the solid lines in Fig. 5. The small J value is rationalized by the fact that a σ–σ superexchange to induce the antiferromagnetic interaction is not possible when the imidazolate group bridges two copper(II) ions at their axial sites.[14] The present J value is smaller than that of **1b** having an imidazolate-bridged helical linear-chain structure ($J = -15$ cm^{-1}).[6a]

The μ_{eff} of complex **3b** is 1.56 μ_B at 290 K which is smaller than the spin-only value of 1.73 μ_B for $S = \frac{1}{2}$. As the temperature is lowered, μ_{eff} decreases to 0.46 μ_B at 44 K. The χ_A *vs.* T curve showed a maximum at 140 K. The magnetic susceptibility data were interpreted quantitatively using equation (2) ($K = J/kT$)

$$\chi_A = \frac{Ng^2\beta}{2kT}\cdot\frac{2 + 5e^{2K} + e^{-2K}}{7 + 5e^{2K} + 3e^{-2K} + e^{-4K}} + N_\alpha \qquad (2)$$

derived from the spin Hamiltonian $H = -2J(S_1 \cdot S_2 + S_2 \cdot S_3 + S_3 \cdot S_4 + S_4 \cdot S_1)$ based on a cyclic tetranuclear structure.[5] The best-fit parameters $J = -60.0$ cm^{-1}, $g = 2.04$, and $R = 9.31 \times 10^{-3}$ were obtained, and the theoretical χ_A and μ_{eff} curves with the fitting parameters are represented by the solid lines in Fig. 6. It should be noted that a fitting procedure based on the Bleaney–Bowers equation (binuclear structure) gave a poorer result. The J value is compatible with those of binuclear copper(II) complexes in which an imidazolate group bridges two copper(II) ions at their equatorial sites.[15] The fairly large antiferromagnetic interaction is explained by the σ–σ superexchange mechanism,[14] since the unpaired electrons of two neighbouring copper(II) ions occupy the orbitals lying in the basal co-ordination planes and can exchange through the imidazolate group. The difference between **2b** and **3b** in the amplitude of antiferromagnetic interaction can be ascribed to the difference in bridging modes.

Conclusion

A method of molecular design of self-assembling metal complexes is described. Mononuclear copper(II) complexes **2a** and **3a** can be modular building blocks in self-assembly reactions because they both have a donor atom to co-ordinate another metal ion and at the same time have an unoccupied or substitutable co-ordination site to receive a donor atom. Under acidic conditions, **2a** and **3a** assume a monomeric structure, whereas under basic conditions a self-assembly reaction is induced by deprotonation of the imidazole proton of the multidentate ligand. The resulting self-assembled structures **2b** and **3b** can be rationalized by co-ordinative demands of the ligand framework and metal co-ordination geometry. The pH titration study of a **3a** indicated that the construction of the self-assembled molecule and its disassembly can occur reversibly. Studies on self-assembled molecules exhibiting functions are now in progress in our laboratory.

Acknowledgements

This work was supported in part by a Grant-in-Aid for Scientific Research from the Ministry of Education, Science, and Culture (Nos. 01540515 and 04453048).

References

1 P. R. Ashton, D. Philip, N. Spencer and J. F. Stoddart, *J. Chem. Soc., Chem. Commun.*, 1992, 1124.
2 J.-M. Lehn, *Angew. Chem., Int. Ed. Engl.*, 1990, **29**, 1304; J.-M. Lehn, A. Rigault, J. Siegel, J. Harrowfield, B. Chevrier and D. Moras, *Proc. Natl. Acad. Sci. USA*, 1987, **84**, 2565; A. Pfeil and J.-M. Lehn, *J. Chem. Soc., Chem. Commun.*, 1992, 838; O. J. Gelling, F. Bolhuis and B. L. Fering, *J. Chem. Soc., Chem. Commun.*, 1991, 917.
3 E. C. Constable and M. D. Ward, *J. Am. Chem. Soc.*, 1990, **112**, 1256; E. C. Constable, *Nature (London)*, 1990, **346**, 314; E. C. Constable, M. G. B. Drew and M. D. Ward, *J. Chem. Soc., Chem. Commun.*, 1987, 1600; E. C. Constable, S. M. Elder, J. Healy and M. D. Ward, *J. Am. Chem. Soc.*, 1990, **112**, 4590; E. C. Constable, M. D. Ward and D. A. Tocher, *J. Chem. Soc., Dalton Trans.*, 1991, 1675; C. J. Cathey, E. C. Constable, M. J. Hannon, D. A. Tocher and M. D. Ward, *J. Chem. Soc., Chem. Commun.*, 1990, 621.
4 D. M. L. Goodgame, D. J. Williams and R. E. P. Winpenny, *J. Chem. Soc., Dalton Trans.*, 1989, 1439; D. M. L. Goodgame, A. M. Khaled, C. A. O'Mahoney and D. J. Williams, *J. Chem. Soc., Chem. Commun.*, 1990, 851; L. H. Carrad, D. M. L. Goodgame and D. J. Williams, *J. Chem. Soc., Chem. Commun.*, 1991, 175.
5 Y. Nakano, W. Mori, N. Okuda and A. Nakahara, *Inorg. Chim. Acta*, 1979, **35**, 1.
6 (*a*) N. Matsumoto, S. Yamashita, A. Ohyoshi, S. Kohata and H. Okawa, *J. Chem. Soc., Dalton Trans.*, 1988, 1943; (*b*) N. Matsumoto, T. Akui, H. Murakami, J. Kanesaka, A. Ohyoshi and H. Okawa, *J. Chem. Soc., Dalton Trans.*, 1988, 1021.
7 *Organic Synthesis*, Wiley, New York, 1955, coll. vol. 3, p. 460; R. A. Turner, C. F. Heubner and C. R. Scholz, *J. Am. Chem. Soc.*, 1949, **71**, 2802; E. P. Papadopolulos, A. Jarrar and C. H. Issidorides, *J. Org. Chem.*, 1966, **31**, 615.
8 L. Sacconi and I. Bertini, *Inorg. Chem.*, 1966, **5**, 1520.
9 R. R. Gagne, *J. Am. Chem. Soc.*, 1976, **98**, 6709.
10 E. A. Boudreaux and L. N. Mulay, *Theory and Application of Molecular Paramagnetism*, Wiley, New York, 1976, p. 491.
11 *International Tables for X-Ray Crystallography*, Kynoch Press, Birmingham, 1974, vol. 4.
12 (*a*) T. Sakurai and K. Kobayashi, *Rikagaku Kenkyusho Hokoku*, 1979, **55**, 69; (*b*) S. Kawano, *Rep. Comput. Cent., Kyushu Univ.*, 1980, **13**, 39; (*c*) C. K. Johnson, ORTEP, Report ORNL no. 3794, Oak Ridge National Laboratory, Oak Ridge, TN, 1965.
13 E. Sinn, *Coord. Chem. Rev.*, 1970, **5**, 313.
14 S. Ohkubo, K. Inoue, H. Tamaki, M. Ohba, N. Matsumoto, H. Ōkawa and S. Kida, *Bull. Chem. Soc. Jpn.*, 1992, **65**, 1603; O. Kahn, *Struct. Bonding (Berlin)*, 1987, **68**, 89; C. J. Cairns and D. H. Busch, *Coord. Chem. Rev.*, 1986, **69**, 1.
15 N. Matsumoto, H. Murakami, T. Akui, J. Honbo, H. Ōkawa and A. Ohyoshi, *Bull. Chem. Soc. Jpn.*, 1986, **59**, 1609; P. Chaudhuri, I. Karpenstein, M. Winter, C. Butzlaff, E. Bill, A. X. Trautwein, U. Florke and H.-J. Haupt, *J. Chem. Soc., Chem. Commun.*, 1992, 321; J. C. Dewan and S. L. Lippard, *Inorg. Chem.*, 1980, **19**, 2079; C. Benelli, R. K. Bunting, D. Gatteschi and C. Zanchini, *Inorg. Chem.*, 1984, **23**, 3074.

Received 9th *March* 1993; *Paper* 3/01403G